E7-2026-18

A. V. Isaev [1,2,*], R. S. Mukhin [1], A. V. Andreev [1],
A. Rahmatinejad [1], T. M. Shneidman [1], H. M. Devaraja [1,2],
M. A. Bychkov [1], M. L. Chelnokov [1], V. I. Chepigin [1],
V. D. Danilkin [1], I. N. Izosimov [1], D. E. Katrasev [1],
A. A. Kuznetsova [1], O. N. Malyshev [1], Yu. A. Popov [1],
A. G. Popeko [1], B. Sailaubekov [1,2], E. A. Sokol [1],
E. Teymurov [1], M. S. Tezekbayeva [1,2], I. I. Ulanova [1],
A. I. Svirikhin [1,2]

AVERAGE NUMBER OF PROMPT NEUTRONS IN THE SPONTANEOUS FISSION OF ^{260}Rf

Submitted to "The European Physical Journal A"

[1] Joint Institute for Nuclear Research, Dubna 141980, Russia
[2] Institute of Nuclear Physics, Almaty 050032, Kazakhstan
[*] E-mail: isaev@jinr.ru

Исаев А. В. и др. E7-2026-18

Среднее число мгновенных нейтронов при спонтанном делении ^{260}Rf

Экспериментальное исследование изотопа ^{260}Rf, образующегося в реакции полного слияния $^{238}\mathrm{U} + {}^{26}\mathrm{Mg}$, выполнено с использованием фильтра скоростей SHELS. Множественность мгновенных нейтронов при спонтанном делении ^{260}Rf измерена впервые, среднее число нейтронов в акте деления данного изотопа составило $\overline{\nu}(^{260}\mathrm{Rf}) = 4{,}88 \pm 0{,}24$. Период полураспада был измерен при доверительном интервале 95 % как $T_{1/2}(^{260}\mathrm{Rf}) = 16{,}8^{+5{,}5}_{-3{,}8}$ мс.

Работа выполнена в Лаборатории ядерных реакций им. Г. Н. Флерова ОИЯИ.

Препринт Объединенного института ядерных исследований. Дубна, 2026

Isaev A. V. et al. E7-2026-18

Average Number of Prompt Neutrons in the Spontaneous Fission of ^{260}Rf

An experimental study of ^{260}Rf produced in the complete fusion reaction $^{238}\mathrm{U} + {}^{26}\mathrm{Mg}$ was performed using the SHELS velocity filter. The prompt neutron multiplicity in the spontaneous fission of ^{260}Rf was measured for the first time, yielding an average value $\overline{\nu}(^{260}\mathrm{Rf}) = 4.88 \pm 0.24$. The half-life was measured as $T_{1/2}(^{260}\mathrm{Rf}) = 16.8^{+5.5}_{-3.8}$ ms (95% CL).

The investigation has been performed at the Flerov Laboratory of Nuclear Reactions, JINR.

Preprint of the Joint Institute for Nuclear Research. Dubna, 2026

INTRODUCTION

Spontaneous fission (SF) of heavy and superheavy nuclei provides direct information on the scission configurations, which result from the interplay between Coulomb repulsion and shell effects. The probabilities of various scission configurations shape the distributions of fragment mass, the total kinetic energy (TKE) and the excitation energy, and, as a result, the subsequent emission of prompt neutrons and γ rays.

From actinides to transfermium and superheavy nuclei, the fission mechanism undergoes qualitative changes with increasing fissility. In actinides, asymmetric fission is strongly influenced by the interplay between the macroscopic part of the potential energy surface (PES) and quantum shell effects. As the fissility parameter Z^2/A increases, the macroscopic PES flattens, thus favoring more compact scission configurations; together with the evolution of fragment shell structure, this contributes to a gradual shift toward more symmetric mass splits. In superheavy nuclei, where stability is largely provided by shell effects, microscopic contributions play a decisive role in shaping the fission barrier and determining the preferred fission path.

A comprehensive description of SF therefore requires the combined analysis of fragment mass distributions, TKE, and prompt neutron emission. Mass distributions reflect shell effects at large deformations, TKE constrains the compactness of the scission configurations, and the average neutron multiplicity ($\overline{\nu}$) provides a sensitive probe of the excitation energy and deformation carried by the fragments. Systematic measurements of $\overline{\nu}$ thus yield important information on how excitation energy is partitioned and on the fission dynamics near scission.

Experimental information on prompt neutron emission in the transfermium and superheavy region remains scarce. To enable studies of nuclei produced at extremely low rates, the high-efficiency SFiNx detector was developed [1, 2]. The detector design enables efficient detection of SF events with reliable event-by-event background evaluation, making it well suited for studies of nuclei produced at the limits of experimental reach. This approach has been successfully applied to isotopes with $Z \geqslant 100$ in complete-fusion (CF) reactions [3–6], as well as to SF shape isomers of lighter actinides ($Z < 100$) populated in multinucleon-transfer (MNT) reactions [7].

Rutherfordium ($Z = 104$) occupies a key position in the transitional region between nobelium and seaborgium isotopes, where the fission mode evolves from predominantly asymmetric to increasingly symmetric or bimodal behavior. TKE distributions have been reported for ^{255,256,258}Rf [8], ^{260}Rf [9],

and ^{262}Rf [10], while fragment mass data for ^{256,258,260,262}Rf are summarized in [10]. Prompt neutron multiplicities have been measured only for neutron-deficient isotopes ^{254}Rf [11] and ^{256}Rf [12], with a complete lack of data for more neutron-rich isotopes including ^{260}Rf.

Therefore, the first measurement of $\overline{\nu}(^{260}\mathrm{Rf})$ provides new experimental input for the systematics of prompt neutron emission in the transfermium region.

1. EXPERIMENTAL DETAILS

An experiment aimed at studying the SF properties of ^{260}Rf was performed at FLNR using the SHELS separator [13] and the SFiNx detection system [2] (Fig. 1). The detection system includes 116 ^{3}He neutron counters capable of detecting multiple prompt neutrons emitted during the SF process, as well as a well-type assembly of double-sided silicon detectors (DSSD), consisting of a 128×128-strip focal-plane detector and eight tunnel detectors with 16×16 strips each, used to register fission fragments and α particles. The single neutron detection efficiency, calibrated with a ^{248}Cm source, was $(56.8 \pm 1)\%$, and the average neutron lifetime in the detector array was (19 ± 1) μs. The high granularity of the SFiNx neutron detector minimizes the probability that more than one neutron is registered in a single ^{3}He counter within the coincidence window [1]. Importantly, the SFiNx operates in a continuous monitoring mode, recording all neutrons independently of any fission trigger, which enables precise event-by-event background evaluation. The DSSD energy calibration for α particles was carried out using the $^{198}\mathrm{Pt}(^{26}\mathrm{Mg}, xn)^{224-x}\mathrm{Th}$ reactions. The detection efficiency of the focal-plane silicon detector is approximately 50% for α particles and nearly 100% for at least one of the two fission fragments.

Before implantation into the focal-plane DSSD, evaporation residues (ERs) traversed a single foil of the time-of-flight (ToF) system [14], which was used to distinguish implantation events from subsequent decays registered in the focal-plane detector. Owing to the low velocities of the ERs produced in the studied reaction, only one ToF foil was installed in order to minimize additional energy loss and avoid a reduction of the decay statistics.

Nine CLLBC-based scintillator detectors were installed directly after the focal-plane DSSD to register prompt γ rays accompanying fission, which can be used in subsequent correlation analysis. The SFiNx detector system was placed behind a wall of heavy concrete about 2 m thick to reduce neutron and gamma backgrounds.

The ^{260}Rf isotope was synthesized in the CF reaction of ^{26}Mg ions from the U-400 cyclotron with a $^{238}\mathrm{U_3O_8}$ target. A 150-mm-diameter target with a thickness of (287 ± 50) μg/cm^2 (^{238}U enrichment about 99.999%) was electrochemically deposited on 1.5-μm-thick Ti backing foil. Measurements were performed at beam energies corresponding to the center of the target in the range 128–134.5 MeV, chosen near the maximum of the excitation function for the $4n$ evaporation channel of the $^{238}\mathrm{U} + ^{26}\mathrm{Mg}$ complete fusion

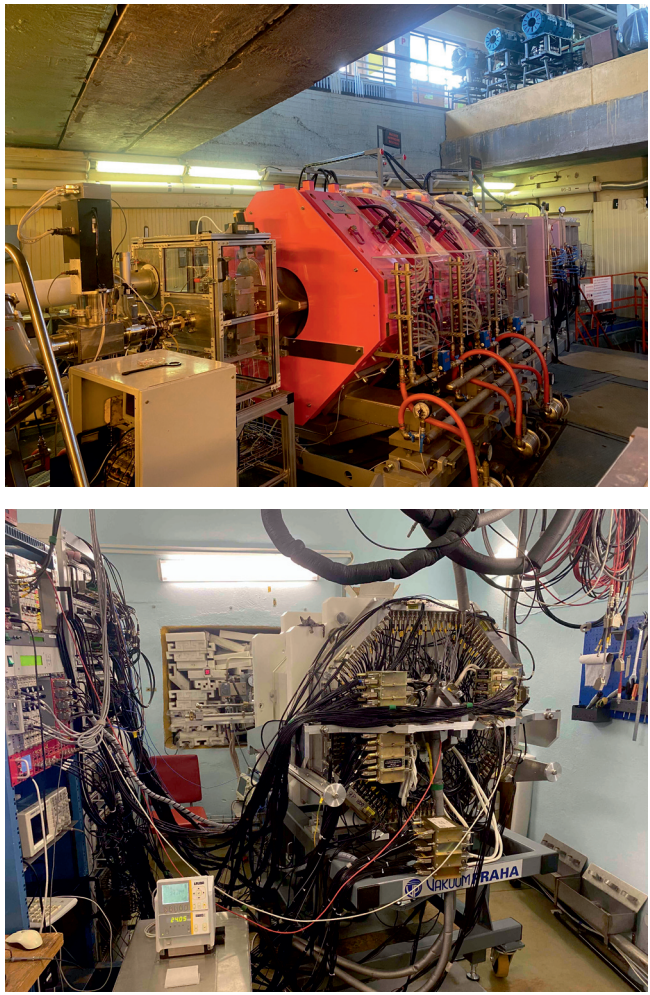

Fig. 1. Upgraded SHELS separator (top), including a new triplet of magnetic quadrupole lenses and a new target box, and the SFiNx detector system (bottom) installed at the focal plane of the separator

reaction [15, 16]. Despite the ^{238}U enrichment of the target being close to 100%, the uranium target contained an impurity of ^{198}Pt resulting from the target fabrication procedure, in which platinum electrodes were used. This impurity significantly affected the analysis of the α spectra, as reactions on platinum produced α lines in the energy region around 9 MeV, overlapping with the α decays of rutherfordium. For this reason, a reliable analysis of α-decay correlations was not pursued in the present work.

In addition to the CF reaction, MNT channels in the $^{238}U + ^{26}Mg$ system were investigated. These reactions are known to populate actinide nuclei in the Am–Pu region, where spontaneously fissioning shape-isomeric states have been reported [17, 18]. MNT products predominantly arise from damped binary collisions and, in near-barrier interactions, target-like fragments are typically characterized by laboratory-frame velocities exceeding those of CF recoils [19].

Calculations indicate that such target-like MNT products attain velocities of approximately 1.3–1.8 v_{CN}, where v_{CN} denotes the compound-nucleus velocity. These estimates were used to define the high-voltage (HV) settings of the SHELS velocity filter. The resulting experimental separation between the CF and MNT velocity regimes is illustrated in Fig. 2. By tuning the HV of the velocity-filter deflectors, the transmission was optimized for CF recoils, while most of the faster transfer products were effectively suppressed. All other separator parameters, including the magnetic dipole and quadrupole fields, were kept unchanged, while only the high voltages applied to the electrostatic deflectors were varied. This significantly reduced the MNT-related background in the CF mode and enabled a dedicated study of prompt-neutron emission from spontaneously fissioning isomers produced in transfer reactions [7]. Nevertheless, a small fraction of transfer products resulting

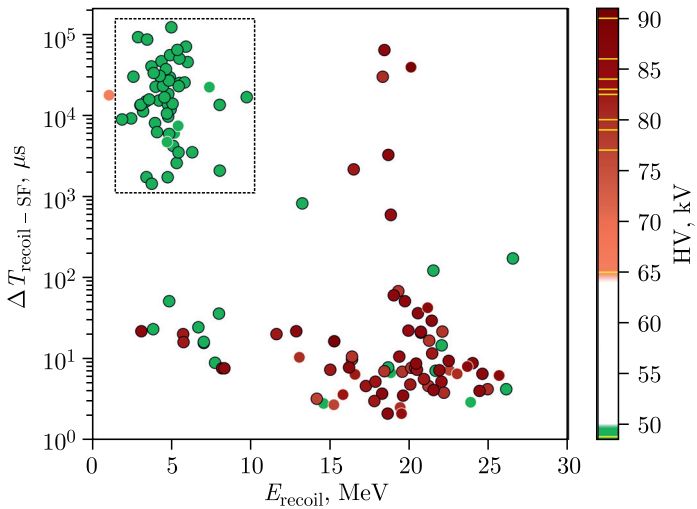

Fig. 2. Distribution of time differences between recoil implantation and fission-fragment detection as a function of recoil energy. Green markers indicate events found in the CF velocity mode of the SHELS separator (HV = 49 kV), while red markers represent events corresponding to the transfer-product velocity regime (HV = 65–90 kV). Thin yellow lines on the colorbar show the exact HV operating modes of the separator used in the experiment. Markers with black borders indicate events with at least one detected prompt neutron. Dashed box represents the CF cluster of ^{260}Rf

from orbiting or highly dissipative collisions may still fall within the velocity range of the CF recoils. The possible contribution of such events is discussed below.

Before entering the velocity filter, the recoils passed through a thin carbon foil to achieve charge-state equilibration. Using the semi-empirical Nikolaev–Dmitriev parameterization [20], the mean equilibrium charge state of ^{26}Mg was estimated to be $\langle q \rangle \approx +11$. The effective width of the charge-state distribution is on the order of one charge unit. The total number of projectiles delivered to the target, as measured with a Faraday cup, was approximately $1.4 \cdot 10^{19}$ and $2.7 \cdot 10^{17}$ for the CF and MNT reaction studies, respectively.

2. RESULTS

A total of 53 SF events of ^{260}Rf were identified. The search was performed within a 100 μs–250 ms time window following implantation signals of recoils with energy $\leqslant$11 MeV. The energy of the fission fragments was required to exceed 30 MeV. SF events were accepted only if accompanied by either a coincident signal from a second fragment in the side detectors or prompt γ rays in the scintillation detectors.

The lower time limit of 100 μs and the upper recoil energy limit of 11 MeV were chosen to exclude products from MNT reactions (Fig. 2).

Prompt neutrons were searched for in the time interval 0–128 μs after the fission signal in the focal-plane Si detector. A total of 147 prompt neutrons in coincidence with 53 fission events attributed to ^{260}Rf were registered. The distribution of the 53 recorded fission events as a function of neutron multiplicity ν is given in the table.

After correction for the neutron detection efficiency of $(56.8 \pm 1.0)\%$, the neutron emission distribution yields an average multiplicity of $\overline{\nu}(^{260}\mathrm{Rf}) = 4.88 \pm 0.24$. The quoted uncertainty includes both statistical and systematic contributions.

Background neutrons were studied by analyzing 10 000 time windows 128 μs in length starting at 1000 μs from each fission event. Owing to the continuous, trigger-independent operation mode of the SFiNx detector,

Observed number of SF events (N) for ^{260}Rf and background neutron probabilities (b_ν), categorized by the number of detected neutrons

ν	N	b_ν
0	4	0.993
1	5	0.007
2	16	$5 \cdot 10^{-5}$
3	12	0
4	9	0
5	5	0
6	1	0
7	1	0

these time windows provide a reliable estimate of the neutron background on an event-by-event basis. In such a data acquisition scheme, background time windows can, in principle, be chosen either before or after the fission event; in the present analysis, post-fission windows were used in order to provide a straightforward and transparent background evaluation. The start time of these background search gates (1000 μs) was selected to minimize overlap with prompt neutrons. The resulting background distribution (Table) was used in the correction procedure. The average background multiplicity was 0.007 neutrons per fission, resulting in a negligible effect on the prompt neutron multiplicity distribution.

After applying the recoil-energy selection of $E_{\text{recoil}} \leqslant 11$ MeV to events in the CF velocity mode of the SHELS separator, two distinct activities are observed (Fig. 3): a long-lived component attributed to the spontaneous fission of ^{260}Rf and a short-lived component described below. The half-life of ^{260}Rf was determined as $T_{1/2}(^{260}\text{Rf}) = 16.8^{+5.5}_{-3.8}$ ms (95% CL) using a maximum-likelihood estimator applied to lifetimes from the recoil–SF correlations. The obtained half-life value of ^{260}Rf agrees with previously reported values of (21 ± 1) ms [9, 21] and $22.2^{+3.0}_{-2.4}$ ms [15].

For spontaneous-fission events correlated with fast recoils ($E > 11$ MeV), attributed to MNT products, the average prompt neutron multiplicity was determined to be 2.4 ± 0.2, based on 71 SF events. A comprehensive investigation of the transfer-induced isomeric states populated in the present experiment, based on the full available statistics, is reported in [7], where an average prompt neutron multiplicity of $\overline{\nu} = 2.65 \pm 0.20$ was obtained; the value measured here is compatible, within uncertainties, with that result.

In addition, a short-lived component was observed in a limited subset (7 events) correlated with slow recoils ($E \leqslant 11$ MeV). Given the very low

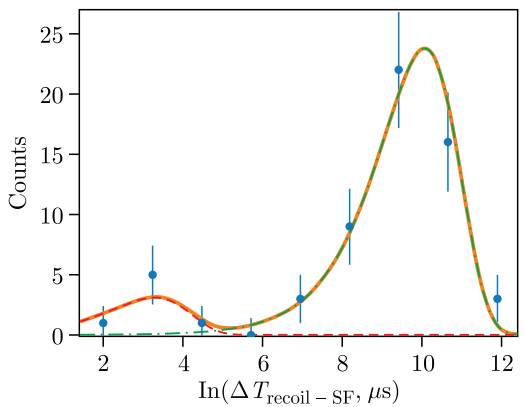

Fig. 3. Distribution of time differences between slow recoil nuclei implantation and fission-fragment detections for events from the CF velocity mode of the separator. The blue points represent the experimental data. The orange solid curve shows the double exponential fit

statistics, no firm conclusion regarding its origin can be drawn; in particular, an assignment to an isomeric state of ^{260}Rf cannot be established on statistical grounds. Therefore, this component is not included in the determination of the average neutron multiplicity of ^{260}Rf reported in this work.

3. DISCUSSION

The systematic behavior of the average prompt-neutron multiplicity as a function of the fissility parameter Z^2/A for nuclides with $Z = 92$–106 is shown in Fig. 4. The value obtained in the present work for ^{260}Rf follows the general increasing trend observed in this region and is consistent with previously measured data for neighboring nuclei.

The reconstructed prompt neutron-emission probability distribution obtained using the Tikhonov regularization method [35, 36] is shown in Fig. 5. Owing to the limited number of detected fission events, the higher moments of the multiplicity distribution (variance and skewness) cannot be reliably determined. Consequently, the reconstructed distribution is presented primarily for illustrative purposes and should be interpreted with caution. Nevertheless, it enables a qualitative comparison with theoretical predictions.

The mass and TKE distributions, as well as neutron multiplicities, were evaluated within the framework of the improved scission model combined with a random-walk treatment of the post-barrier evolution [12, 37, 38]. The results of the calculations are presented in the top, middle, and bottom panels of Fig. 5, respectively. In these calculations, the same parameterization that previously provided a good description of the average neutron multiplicities for Rf and Sg isotopes is used [6].

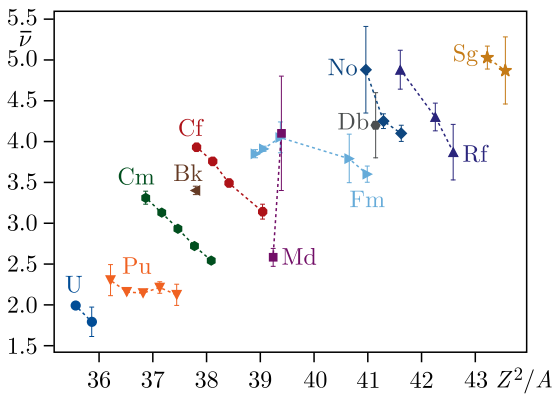

Fig. 4. Average prompt neutron multiplicity vs. the parameter Z^2/A for SF of nuclides with $Z = 92$–106. References: U — [22, 23]; Pu — [24–26]; Cm — [24, 27]; Bk — [27]; Cf — [24, 25, 27, 28]; Fm — [3, 4, 28, 29, 30]; Md — [31, 32]; No — [1, 5, 33]; Rf — [11, 12] and current work (the upper point); Db — [34]; Sg — [6]

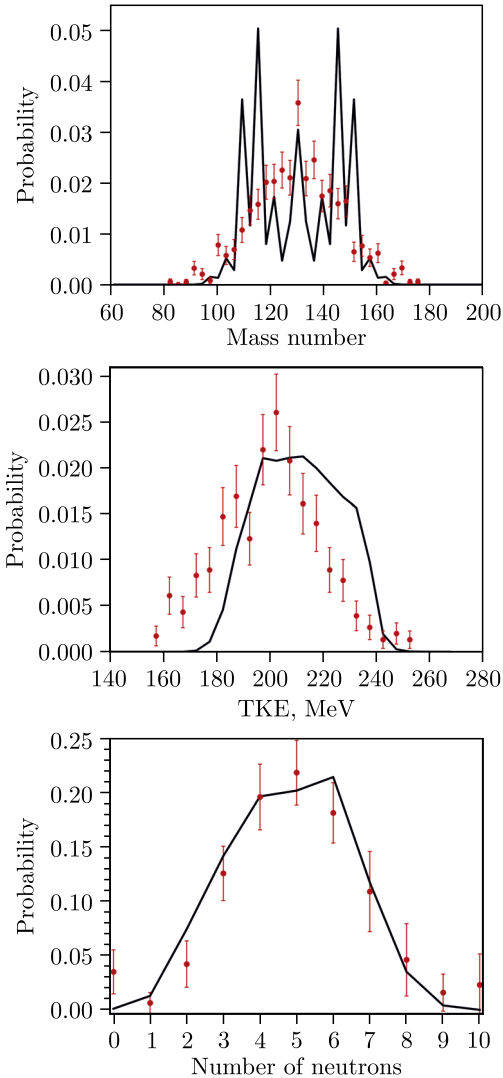

Fig. 5. Calculated mass distributions of fission fragments (top), TKE distributions of the fragments (middle), and prompt neutron multiplicity distribution (bottom) for the spontaneous fission of ^{260}Rf (black solid lines) obtained within the improved scission-point model [37–40]. Experimental data for fragment masses and TKE (red circles with statistical error bars) are taken from [9] and correspond to post-neutron fragment quantities reconstructed using the $2E$ method. The experimental prompt neutron emission probability distribution for ^{260}Rf obtained in the present work is also shown (red circles)

In comparison with the mass distribution of ^{260}Sg [6], the symmetric peak in ^{260}Rf appears more pronounced. This peak, corresponding to the $^{130}\mathrm{Te} + {}^{130}\mathrm{Te}$ configuration, is also observed in the experimental data [9]. In the calculations both symmetric and asymmetric fission modes are obtained. However, they appear more clearly separated than in the experimental data [9], where a broad distribution around the symmetric mass split is observed.

The calculated TKE distribution has an average value of 211 MeV and shows a broad maximum around 200 MeV, consistent with the position of the peak observed experimentally [9]. However, the shape of the calculated distribution on the low- and high-energy sides of the peak differs from the experimental one. This discrepancy likely arises from the absence of octupole deformations in the current version of the model (see the discussion in [38]).

For neutron multiplicity, the calculations yield an average value of 4.82, which is consistent with the measured value of 4.88 ± 0.24. The obtained neutron multiplicity distribution reproduces the general shape of the experimental data (see bottom panel of Fig. 5). In particular, while the distribution for ^{260}Sg is skewed toward higher multiplicities around $\nu \sim 6$ [6], the calculated distribution for ^{260}Rf exhibits a broader maximum around $\nu \sim 5$.

4. CONCLUSIONS

The average prompt neutron multiplicity in the spontaneous fission of ^{260}Rf has been measured for the first time. From 53 identified fission events, the mean multiplicity was determined as $\overline{\nu}(^{260}\mathrm{Rf}) = 4.88 \pm 0.24$. The half-life of ^{260}Rf was obtained as $T_{1/2}(^{260}\mathrm{Rf}) = 16.8^{+5.5}_{-3.8}$ ms (95% CL), in agreement with previously reported values.

The measured value of $\overline{\nu}$ follows the established systematic trend with the fissility parameter Z^2/A for transfermium nuclei. The result is reproduced within uncertainties by calculations performed in the framework of the improved scission-point model. Only the average number of neutrons per fission event could reliably be determined within the given sample size; more data is required to make decisions on distribution shape or higher-order moments.

A key element enabling this measurement was the velocity-based separation of complete-fusion and multinucleon-transfer products with the upgraded SHELS filter. The controlled suppression of background from multinucleon-transfer reactions made it possible to isolate spontaneous-fission events of ^{260}Rf. This capability is essential for extending prompt-neutron studies to nuclei produced with extremely low cross sections in heavy-ion reactions.

The SFiNx detector system proves effective for systematic studies of spontaneous fission in heavy and superheavy nuclei and is suitable for use at the SHE Factory at JINR [41].

Funding. This work was supported by the Science Committee of the Ministry of Science and Higher Education of the Republic of Kazakhstan (Grant No. AP26195449).

Acknowledgements. The authors express their deep gratitude to the U-400 cyclotron team for providing high-quality ^{26}Mg beam.

REFERENCES

1. *Isaev A. V. et al.* The SFiNx Detector System // Phys. Part. Nucl. Lett. 2022. V. 19, No. 1. P. 37–45; DOI: 10.1134/s154747712201006x.
2. *Isaev A. V. et al.* The SFiNx Detector System (Current Status) // Phys. Part. Nucl. Lett. 2025. V. 22, No. 2. P. 300–303; DOI: 10.1134/S1547477124702303.
3. *Mukhin R. S. et al.* Prompt Neutron Multiplicity from Spontaneous Fission of ^{244}Fm // Eur. Phys. J. A. 2024. V. 60, No. 11. P. 223; DOI: 10.1140/epja/s10050-024-01441-0.
4. *Isaev A. V. et al.* Prompt Neutron Emission in the Spontaneous Fission of ^{246}Fm // Eur. Phys. J. A. 2022. V. 58, No. 6. P. 108; DOI: 10.1140/epja/s10050-022-00761-3.
5. *Mukhin R. S. et al.* Prompt Neutron Emission in ^{250}No Spontaneous Fission Associated with Ground and Isomeric State Decays // Chin. Phys. C. 2024. V. 48, No. 6. 064002; DOI: 10.1088/1674-1137/ad361a.
6. *Isaev A. V. et al.* Prompt Neutron Emission in the Spontaneous Fission of $^{258, 260}$Sg // Phys. Rev. C. 2026 (submitted).
7. *Sailaubekov B. et al.* First Investigation of Prompt Neutrons from Spontaneously Fissioning Isomers Produced in Multinucleon Transfer Reactions // Phys. Lett. B. 2026. V. 872. 140071; DOI: https://doi.org/10.1016/j.physletb.2025.140071. URL: https://www.sciencedirect.com/science/article/pii/ S0370269325008299.
8. *Mosat P. et al. K* Isomerism in ^{255}Rf and Total Kinetic Energy Measurements for Spontaneous Fission of $^{255, 256, 258}$Rf // Phys. Rev. C. 2020. V. 101. 034310; DOI: 10.1103/PhysRevC.101.034310.
9. *Hulet E. K. et al.* Spontaneous Fission Properties of ^{258}Fm, ^{259}Md, ^{260}Md, ^{258}No, and ^{260}[104]: Bimodal Fission // Phys. Rev. C. 1989. V. 40. P. 770–784; DOI: 10.1103/PhysRevC.40.770.
10. *Lane M. R.* Spontaneous Fission of the Heaviest Elements. PhD thesis. Lawrence Berkeley National Laboratory. Berkeley, 1999.
11. *Svirikhin A. I. et al.* Prompt Neutrons from Spontaneous ^{254}Rf Fission // Phys. Part. Nucl. Lett. 2019. V. 16, No. 6. P. 768–771; DOI: 10.1134/ s1547477119060311.
12. *Isaev A. V. et al.* Structure of the Prompt Neutron Multiplicity Distribution in the Spontaneous Fission of ^{256}Rf // Phys. Lett. B. 2023. V. 843. 138008; DOI: 10.1016/j.physletb.2023.138008.
13. *Popeko A. G. et al.* Separator for Heavy ELement Spectroscopy — Velocity Filter SHELS // Nucl. Instr. Meth. B. 2016. V. 376. P. 140–143; DOI: 10.1016/j.nimb. 2016.03.045.
14. *Andreyev A. N. et al.* Large Area High-Efficiency Time-of-Flight System for Detection of Low Energy Heavy Evaporation Residues at the Electrostatic

Separator VASSILISSA // Nucl. Instr. Meth. A. 1995. V. 364, No. 2. P. 342–348; DOI: 10.1016/0168-9002(95)00355-X.

15. *Gates J. M. et al.* Synthesis of Rutherfordium Isotopes in the ^{238}U(^{26}Mg, xn)$^{264-x}$Rf Reaction and Study of Their Decay Properties // Phys. Rev. C. 2008. V. 77. 034603; DOI: 10.1103/PhysRevC.77.034603.
16. *Gregorich K. et al.* Heavy Element Formation in Compound Nucleus Reactions with ^{238}U Targets. Tech. rep. LBNL-63617. OSTI ID: 1735553. Peer-reviewed. Available at: https://escholarship.org/uc/item/0td0f61k. Lawrence Berkeley National Laboratory, 2023.
17. *Polikanov S. M.* Spontaneously Fissioning Isomers // Phys. Usp. 1968. V. 11, No. 1. P. 22–33; DOI: 10.1070/PU1968v011n01ABEH003722; URL: https://ufn.ru/en/articles/1968/1/b/.
18. *Leoni S. et al.* Shape Isomers: Status and Perspectives across the Nuclear Chart // Eur. Phys. J. Special Topics 2024. V. 233, No. 5. P. 1061–1074; DOI: 10.1140/epjs/s11734-024-01175-6.
19. *Devaraja H. M. et al.* Systematic Studies to Produce Heavy Above-Target Nuclides in Multinucleon Transfer Reactions // Phys. Lett. B. 2025. V. 862. 139353; DOI: https://doi.org/10.1016/j.physletb.2025.139353; URL: https://www.sciencedirect.com/science/article/pii/S0370269325001133.
20. *Nikolaev V. S., Dmitriev I. S.* On the Equilibrium Charge Distribution in Heavy Element Ion Beams // Phys. Lett. A. 1968. V. 28, No. 4. P. 277–278; DOI: 10.1016/0375-9601(68)90282-X. URL: https://www.sciencedirect.com/science/article/pii/037596016890282X.
21. *Somerville L. P. et al.* Spontaneous Fission of Rutherfordium Isotopes // Phys. Rev. C. 1985. V. 31. P. 1801–1815; DOI: 10.1103/PhysRevC.31.1801.
22. *Popeko A. G. et al.* Multiplicity of Prompt Neutrons in Spontaneous Fission of ^{238}U // Sov. J. Nucl. Phys. 1976. V. 24, No. 3. P. 245–247.
23. *Belenkii S. N., Skorokhvatov M. D., Etenko A. V.* Measurement of the Characteristics of Spontaneous Fission of ^{238}U and ^{236}U // Sov. At. Energy. 1983. V. 55, No. 2. P. 528–530; DOI: 10.1007/bf01138346.
24. *Orth C. J.* The Average Number of Neutrons Emitted in the Spontaneous Fission of Some Even–Even Heavy Nuclides // Nucl. Sci. Engin. 1971. V. 43, No. 1. P. 54–57; DOI: 10.13182/nse71-a21245.
25. *Lazarev Yu. A.* Variance of the Energy Distributions of Fragments Formed by Low-Energy Fission: Experimental Data and Theoretical Predictions // At. Energy Rev. 1977. V. 15, No. 1. P. 75–107.
26. *Boldeman J. W.* Prompt ν Measurements for the Spontaneous Fission of ^{240}Pu and ^{242}Pu // J. Nucl. Energy. 1968. V. 22, No. 2. P. 63–72; DOI: 10.1016/0022-3107(68)90055-5.
27. *Holden N. E., Zucker M. S.* Prompt Neutron Multiplicities for the Transplutonium Nuclides // Radiation Effects. 1986. V. 96, No. 1–4. P. 289–292; DOI: 10.1080/00337578608211755.
28. *Hoffman D. C. et al.* Neutron Multiplicity Measurements of Cf and Fm Isotopes // Phys. Rev. C. 1980. V. 21, No. 2. P. 637–646; DOI: 10.1103/PhysRevC.21.637.
29. *Sokol E. A., Zeinalov Sh. S., Ter-Akopian G. M.* Multiplicity of Fast Neutrons in the Spontaneous Fission of ^{256}Fm // Sov. At. Energy. 1989. V. 67, No. 5. P. 851–852; DOI: 10.1007/bf01126141.

30. *Choppin G. R. et al.* Prompt Neutrons from the Spontaneous Fission of Fermium-254 // Phys. Rev. 1956. V. 102, No. 3. P. 766–766; DOI: 10.1103/PhysRev.102.766.
31. *Wild J. F. et al.* Prompt Neutron Emission from the Spontaneous Fission of ^{260}Md // Phys. Rev. C. 1990. V. 41, No. 2. P. 640–646; DOI: 10.1103/PhysRevC.41.640.
32. *Ter-Akopyan G. M., Buklanov G. V., Zeinalov Sh. S.* Recording of Multiple Neutron Events, and a Study of Spontaneous Fission of Heavy Nuclei in Experiments on the Synthesis of Superheavy Nuclei and the Search for Them in Nature // Intern. Workshop on the Physics of Heavy Ions. Dubna, 1987. P. 212–216 (in Russian).
33. *Isaev A. V. et al.* Comparative Study of Spontaneous-Fission Characteristics of ^{252}No and ^{254}No Isotopes // Phys. Part. Nucl. Lett. 2021. V. 18, No. 4. P. 449–456; DOI: 10.1134/s1547477121040087.
34. *Oganessian Yu. Ts. et al.* Synthesis of Elements 115 and 113 in the Reaction ^{243}Am + ^{48}Ca // Phys. Rev. C. 2005. V. 72, No. 3. 034611; DOI: 10.1103/PhysRevC.72.034611.
35. *Turchin V. F., Kozlov V. P., Malkevich M. S.* The Use of Mathematical-Statistics Methods in the Solution of Incorrectly Posed Problems // Sov. Phys. Usp. 1971. V. 13, No. 6. P. 681–703; DOI: 10.1070/pu1971v013n06abeh004273.
36. *Mukhin R. S. et al.* Reconstruction of Spontaneous Fission Neutron Multiplicity Distribution Spectra by the Statistical Regularization Method // Phys. Part. Nucl. Lett. 2021. V. 18, No. 4. P. 439–444; DOI: 10.1134/s1547477121040130.
37. *Rahmatinejad A. et al.* Evolution of Fission Properties in Fermium Region // Intern. J. Mod. Phys. E. 2024. V. 33, No. 11. 2441018; DOI: 10.1142/s0218301324410180.
38. *Rahmatinejad A. et al.* Dependence of Angular Momentum of Fission Fragments on Total Kinetic Energy in Spontaneous Fission of ^{252}Cf // Phys. Rev. C. 2025. V. 112, No. 4. 044610; DOI: 10.1103/yklf-mh6w.
39. *Andreev A. V. et al.* Possible Explanation of Fine Structures in Mass-Energy Distribution of Fission Fragments // Eur. Phys. J. A. 2004. V. 22, No. 1. P. 51–60; DOI: 10.1140/epja/i2004-10017-9.
40. *Andreev A. V. et al.* Ternary Fission within Statistical Approach // Eur. Phys. J. A. 2006. V. 30, No. 3. P. 579–589; DOI: 10.1140/epja/i2006-10145-2.
41. *Dmitriev S. N., Itkis M. G., Oganessian Yu. Ts.* Status and Perspectives of the Dubna Superheavy Element Factory // Eur. Phys. J. Web Conf. 2016. V. 131. P. 08001; DOI: 10.1051/epjconf/201613108001.

Received on April 2, 2026.

Редактор *Е. И. Крупко*

Подписано в печать 05.05.2026.
Формат 60 × 90/16. Бумага офсетная. Печать цифровая.
Усл. печ. л. 1,00. Уч.-изд. л. 1,02. Тираж 110 экз. Заказ № 61309.

Издательский отдел Объединенного института ядерных исследований
141980, г. Дубна, Московская обл., ул. Жолио-Кюри, 6.
E-mail: publish@jinr.ru
www.jinr.ru/publish/